The EMBO Journal (2012) 31, 1217–1230 | © 2012 European Molecular Biology Organization | All Rights Reserved 0261-4189/12
www.embojournal.org

THE EMBO JOURNAL

Raising cytosolic Cl^- in cerebellar granule cells affects their excitability and vestibulo-ocular learning

Patricia Seja[1,8], Martijn Schonewille[2,8], Guillermo Spitzmaul[1,8], Aleksandra Badura[2,8], Ilse Klein[3], York Rudhard[3], William Wisden[4], Christian A Hübner[3,5], Chris I De Zeeuw[2,6,*] and Thomas J Jentsch[1,3,7,*]

[1]Leibniz-Institut für Molekulare Pharmakologie (FMP) and Max-Delbrück-Centrum für Molekulare Medizin (MDC), Berlin, Germany, [2]Department of Neuroscience, Erasmus MC, Rotterdam, The Netherlands, [3]Zentrum für Molekulare Neurobiologie (ZMNH), Universität Hamburg, Hamburg, Germany, [4]Molecular Cell Biology, Imperial College, London, UK, [5]Institut für Humangenetik, Universitätsklinikum Jena, Friedrich-Schiller-Universität Jena, Jena, Germany, [6]Netherlands Institute for Neuroscience, Amsterdam, The Netherlands and [7]Cluster of Excellence NeuroCure, Charité-Universitätsmedizin Berlin, Berlin, Germany

Cerebellar cortical throughput involved in motor control comprises granule cells (GCs) and Purkinje cells (PCs), both of which receive inhibitory GABAergic input from interneurons. The GABAergic input to PCs is essential for learning and consolidation of the vestibulo-ocular reflex, but the role of GC excitability remains unclear. We now disrupted the Kcc2 K-Cl cotransporter specifically in either cell type to manipulate their excitability and inhibition by $GABA_A$-receptor Cl^- channels. Although Kcc2 may have a morphogenic role in synapse development, *Kcc2* disruption neither changed synapse density nor spine morphology. In both GCs and PCs, disruption of Kcc2, but not Kcc3, increased $[Cl^-]_i$ roughly two-fold. The reduced Cl^- gradient nearly abolished GABA-induced hyperpolarization in PCs, but in GCs it merely affected excitability by membrane depolarization. Ablation of Kcc2 from GCs impaired consolidation of long-term phase learning of the vestibulo-ocular reflex, whereas baseline performance, short-term gain-decrease learning and gain consolidation remained intact. These functions, however, were affected by disruption of Kcc2 in PCs. GC excitability plays a previously unknown, but specific role in consolidation of phase learning.

The EMBO Journal (2012) **31,** 1217–1230. doi:10.1038/emboj.2011.488; Published online 17 January 2012

*Corresponding authors. CI De Zeeuw, Department of Neuroscience, Erasmus MC, P.O. Box 2040, 3000 CA Rotterdam, The Netherlands. Tel.: +31 10 7043299; Fax: +31 10 7044734; E-mail: c.dezeeuw@erasmusmc.nl; Netherlands Institute for Neuroscience, Meibergdreef 47, 1105 BA Amsterdam, The Netherlands. Tel.: +31 20 5668011; Fax: +31 20 5665500; E-mail: c.de.zeeuw@nin.knaw.nl or TJ Jentsch, Leibniz-Institut für Molekulare Pharmakologie (FMP) and Max-Delbrück-Centrum für Molekulare Medizin (MDC), Robert-Rössle-Strasse 10, 13125 Berlin, Germany. Tel.: +49 30 9406 2961; Fax: +49 30 9406 2960; E-mail: jentsch@fmp-berlin.de
[8]These authors contributed equally to this work

Received: 28 June 2011; accepted: 6 December 2011; published online: 17 January 2012

Subject Categories: signal transduction; neuroscience
Keywords: dendritic spine; GABA switch; glycine receptor; potassium-chloride cotransporter; synaptic inhibition

Introduction

The cerebellum controls movements through a uniformly patterned neuronal circuitry in the cerebellar cortex (Figure 1A). GABAergic Purkinje cells (PCs) provide the only output of the cerebellum (Eccles *et al*, 1967). PCs receive excitatory input directly from climbing fibres, and indirectly from mossy fibres through granule cells (GCs) whose axons form the parallel fibre system. The activity of PCs and GCs is controlled by inhibitory GABAergic interneurons, such as stellate, basket, and Golgi cells (De Zeeuw *et al*, 2011). These interneurons are also activated by parallel fibres and give rise to a feedback and feedforward inhibition on GCs through Golgi cells, and to feedforward inhibition on PCs through stellate cells and basket cells (Figure 1A). The role of inhibition on GC output and subsequently motor control remains poorly understood (Gabbiani *et al*, 1994). While feedforward inhibition modulates the timing and pattern of PC activity (Hausser and Clark, 1997; Mittmann and Hausser, 2007; Santamaria *et al*, 2007; Wulff *et al*, 2009), feedback inhibition of GCs is thought to filter their mossy fibre input (Gabbiani *et al*, 1994). The functional roles of specific inhibitory pathways in cerebellar circuits have been probed by elimination of Golgi cells (Watanabe *et al*, 1998) and by genetic disruption of PC $GABA_A$ receptor ($GABA_AR$) subunits (Wulff *et al*, 2009). Elimination of Golgi cells produced severe acute motor disorders (Watanabe *et al*, 1998), whereas chronic Purkinje cell-specific disruption of $\gamma2$ $GABA_AR$ subunits led to mild impairment of baseline motor performance accompanied by a dramatic deficit in motor learning and consolidation of both amplitude and timing parameters (Wulff *et al*, 2009).

Here, we take a different approach by changing the Cl^- equilibrium potential of the two main target cells of synaptic inhibition in the cerebellum. The electrical response of $GABA_ARs$ depends on the difference between the resting membrane potential and the Cl^- equilibrium potential. Neuronal intracellular Cl^- concentration ($[Cl^-]_i$) is mainly determined by the opposing activities of Cl^--extruding K-Cl cotransporters (KCCs) and the Cl^--accumulating Na-K-2Cl cotransporter Nkcc1 (Blaesse *et al*, 2009). The change from perinatal depolarizing GABA response to the hyperpolarizing response in the adult CNS (the 'GABA switch') (Cherubini *et al*, 1991; Ben-Ari *et al*, 1997) is correlated with a down-regulation of Nkcc1 and an upregulation of Kcc2 (Rivera *et al*, 1999; Hübner *et al*, 2001a, b; Stein *et al*, 2004; Pfeffer *et al*, 2009). Kcc2 is neuron specific and broadly expressed across

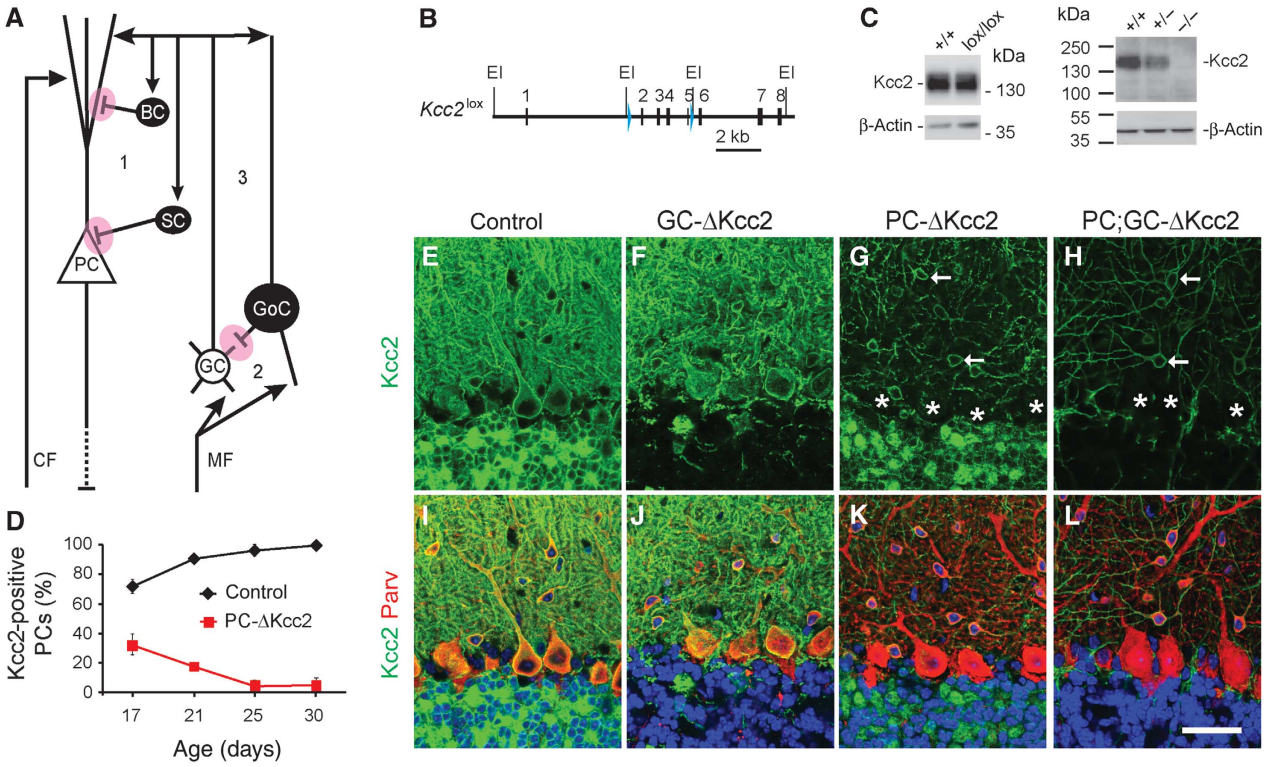

Figure 1 Cell type-specific deletion of *Kcc2* in the cerebellum. (**A**) Cerebellar neuronal circuitry. Input into the cerebellum is through mossy fibres (MFs) and climbing fibres (CFs). GABAergic Purkinje cells (PCs) provide the only output. Inhibitory interneurons (SCs, stellate cells; BCs, basket cells; GoCs, Golgi cells) generate feedforward inhibition on PCs (1) and granule cells (GCs) (2), as well as feedback inhibition on GCs (3). Cell bodies in which *Kcc* genes were deleted are not filled and synapses that are expected to be attenuated in our mouse models are highlighted in pink. (**B**) Targeted allele ($Kcc2^{lox}$) of the *Kcc2* (*Slc12a5*) locus. Exons 2–5 were flanked by loxP sites (arrowheads). Exons are indicated by black bars. E1, *Eco*RI restriction site used for genotyping by Southern blotting. (**C**) Western blots showing that $Kcc2^{lox/lox}$ mice express the Kcc2 protein at WT levels (left) and that the anti-Kcc2 antibody is specific (right; no signal in $Kcc2^{-/-}$ mice). (**D**) Progression of Kcc2 expression on Purkinje cells from $Kcc2^{lox/lox}$ (control) and PC-ΔKcc2 mice, averaged over all regions in the vermis. PCs showing somatic membrane staining were counted as positive cells (average ± standard deviation, $n = 2$, 1, 4, and 2 mice for P17, P21, P25, and P30, respectively (for each genotype); ~200 cells counted per animal). Also in granule cells of the vermis, Kcc2 deletion was complete at P25. (**E**–**L**) Immunofluorescent labelling for Kcc2 (green), parvalbumin (red), and nuclei (blue) (**I**–**L**) on sagittal sections of cerebellar cortex from adult mice (scale bar: 40 μm). (**E**, **I**) $Kcc2^{lox/lox}$ mice (control). (**F**, **J**) GC-ΔKcc2 mice with specific *Kcc2* deletion in granule cells. (**G**, **K**) PC-ΔKcc2 mice with specific deletion of *Kcc2* in Purkinje cells. (**H**, **L**) PC;GC-ΔKcc2 mice with *Kcc2* deletion in both PCs and GCs. Kcc2 expression remains in cerebellar interneurons (**G**, **H**, arrows). Asterisks in (**G**, **H**) indicate PC somata.

the adult CNS (Stein *et al*, 2004). Kcc1 and Kcc3 are also found in brain (Pearson *et al*, 2001; Mikawa *et al*, 2002; Wang *et al*, 2002; Boettger *et al*, 2003), but their contribution to neuronal Cl^- extrusion is unclear (Boettger *et al*, 2003). In the cerebellar cortex, Kcc2 is present in GCs, PCs, and interneurons (Williams *et al*, 1999; Stein *et al*, 2004; Takayama and Inoue, 2006), whereas Kcc3 has been found only on PCs (Pearson *et al*, 2001; Boettger *et al*, 2003). The neuronal expression of Nkcc1 generally decreases postnatally (Hübner *et al*, 2001a; Mikawa *et al*, 2002), but cerebellar GCs retain substantial Nkcc1 expression throughout adulthood (Kanaka *et al*, 2001; Hübner *et al*, 2001a; Mikawa *et al*, 2002).

To explore the role of synaptic inhibition in cerebellar function, we specifically disrupted *Kcc2* in GCs and PCs, and *Kcc3* in PCs. This circumvents the perinatal lethality and CNS degeneration of constitutive *Kcc2* (Hübner *et al*, 2001b) and *Kcc3* (Boettger *et al*, 2003) disruption, respectively, and allows the assignment of phenotypes to specific cell types. Whereas this work identifies Kcc2 as the major Cl^- extruder of both GCs and PCs, the effect of *Kcc2* disruption on the GABA response of either cell type was different. It strongly reduced the GABA-induced hyperpolarization of PCs, but surprisingly the voltage response of GCs remained virtually unchanged. This was a consequence of a constitutive depolarization of $Kcc2^{-/-}$ GCs by Cl^- currents through $GABA_A$Rs and glycine receptors (GlyRs). Possibly caused by an increased excitability of constitutively depolarized GCs, GC-ΔKcc2 mice could not consolidate their phase learning of vestibulo-ocular reflexes. Our work reveals an unexpected role of the $[Cl^-]_i$ of GCs in cerebellar plasticity.

Results

Specific deletion of Kcc2 and Kcc3 in cerebellar GCs and PCs

To allow cell type-specific deletion of the K-Cl-cotransporters Kcc2 and Kcc3, we generated $Kcc2^{lox/lox}$ and $Kcc3^{lox/lox}$ mice in which exons 2–5 and 5–6, respectively, were flanked by loxP sites (Figures 1B and 2A; Materials and methods). $Kcc2^{lox/lox}$ mice expressed Kcc2 at wild-type (WT) levels (Figure 1C) without a change in cellular and subcellular localization (Hübner *et al*, 2001b; Figure 1E and I).

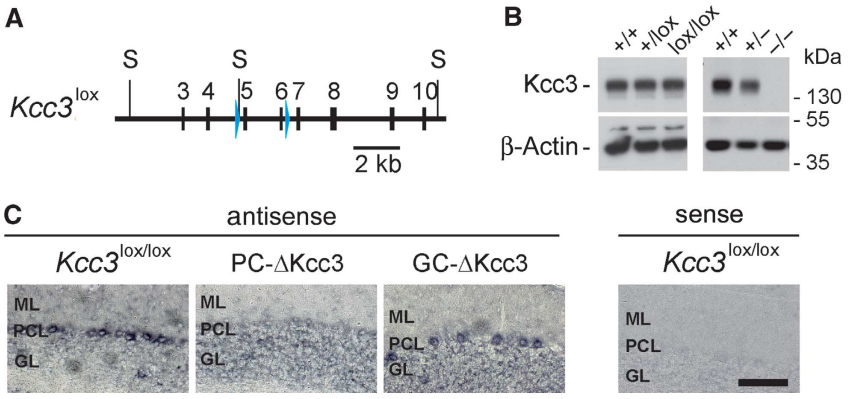

Figure 2 Cell type-specific disruption of *Kcc3* in Purkinje cells. (**A**) Targeted allele ($Kcc3^{lox}$) of the *Kcc3* (*Slc12a6*) locus. Exons 5 and 6 were flanked by loxP sites (arrowheads). Exons are indicated by black bars. S, *Spe*I restriction sites used for genotyping by Southern blotting. (**B**) Western blots showing that $Kcc3^{lox/lox}$ mice express the Kcc3 protein at WT levels and the specificity of the Kcc3 antibody. (**C**) *In-situ* hybridization for *Kcc3* mRNA of sagittal sections of cerebellar cortex from adult control, PC-ΔKcc3, and GC-ΔKcc3 mice. The probe is directed against sequence of exons 5 and 6, which are flanked by loxP sites. Strong hybridization of the antisense probe is observed in Purkinje cells of control and GC-ΔKcc3, but not of PC-Kcc3 mice. The signal in GC-ΔKcc3 mice did not differ from $Kcc3^{lox/lox}$ control. In the granule cell layer, Golgi cells were positive for Kcc3, but no staining could be assigned to granule cells. No staining was observed with the control sense probe on sections from $Kcc3^{lox/lox}$ (control) cerebellum (scale bar: 100 μm).

Likewise, Kcc3 expression levels were normal in $Kcc3^{lox/lox}$ mice (Figure 2B).

These 'floxed' mice were crossed with L7/Pcp2::Cre mice (Barski *et al*, 2000) or with Δα6::Cre mice (Aller *et al*, 2003) to disrupt *Kcc*s specifically in PCs or GCs. These conditional knockout (KO) mice will be named as PC-ΔKcc2, GC-ΔKcc2, PC;GC-ΔKcc2, PC-ΔKcc3, and PC-Δ(Kcc2 + Kcc3) for mice lacking expression of Kcc2 and/or Kcc3 in either PCs or GCs, respectively. These mice survived normally and had no immediately visible phenotype.

Cerebellar expression of Kcc2 increases after birth (Stein *et al*, 2004) and reaches adult levels between P20 and P30 (Figure 1D). Around P30, Kcc2 was robustly expressed in neurons of the cerebellar cortex. Kcc2 expression was specifically lost in GCs of GC-ΔKcc2 mice (Figure 1F and J), and in PCs (marked by asterisks in Figure 1G and H) of PC-ΔKcc2 mice (Figure 1G and K). The combination of both Cre lines deleted Kcc2 from both GCs and PCs (Figure 1H and L), but not from interneurons (Figure 1G and H, arrows). As we lack suitable Kcc3 antibodies for immunohistochemistry, we used *in-situ* hybridization to show prominent *Kcc3* mRNA expression in PCs that was abolished in PC-ΔKcc3, but not in GC-ΔKcc3 mice (Figure 2C).

No change in synaptic morphology and function upon Kcc2 disruption

Changes in intraneuronal Cl^- concentration during postnatal development (the 'GABA switch') are believed to be important for CNS development (Ben-Ari *et al*, 1997; Ben-Ari, 2002). Furthermore, Kcc2 was reported to promote spine development by interacting with the cytoskeleton at synapses (Li *et al*, 2007). However, adult GC-ΔKcc2, PC-ΔKcc2, and PC;GC-ΔKcc2 mice displayed normal cerebellar histology (Supplementary Figure S1) and a normal distribution of inhibitory and excitatory synapses (Figure 3A). Biocytin-filled PCs revealed no difference in morphology and length of dendritic spines between WT and PC;GC-ΔKcc2 (Figure 3B and C). We also did not detect morphological deficits at the ultrastructural level (Figure 3D). The density of inhibitory synapses in the GC and molecular layers (Figure 3E), the density of parallel fibre synapses and the morphology of their PC spines were unchanged (Figure 3F). Consistent with a normal number and function of both inhibitory and excitatory synapses, the frequencies of both miniature inhibitory postsynaptic currents (mIPSCs; Figure 4A) and miniature excitatory postsynaptic currents (mEPSCs; Figure 4B), recorded in the presence of tetrodotoxin (to inhibit action potentials) from PCs of control $Kcc2^{lox/lox}$ and PC-ΔKcc2 mice were undistinguishable. Spontaneous IPCSs (sIPSCs) and EPSCs (sEPSCs) (measured without blockers) are influenced by the spontaneous firing of neurons synapsing on PCs (Figure 1A). Whereas there was no difference in sIPSC frequencies between the genotypes (Figure 4C), the sEPSC frequency of GC-ΔKcc2 PCs was marginally higher ($P = 0.035$) compared with control mice (Figure 4D), hinting at a higher excitability of GCs lacking Kcc2.

Kcc2 is the major Cl^- extruder of PCs

To examine the roles of Kcc2 and Kcc3 in PC Cl^- homeostasis, we measured GABA-induced Cl^- currents using non-invasive gramicidin-perforated patch-clamp technique between P25 and P65 in lobules 4–5 of the vermis when deletion of Kcc2 was complete (Figure 1D).

The $GABA_AR$ agonist muscimol strongly hyperpolarized PCs from (control) $Kcc2^{lox/lox}$ mice. This response was greatly reduced in PC-ΔKcc2 mice (Figure 5A). E_{GABA} was determined from the reversal potential of $GABA_AR$ currents (Figure 5B and C). E_{GABA} of PCs lacking Kcc2 was ∼20 mV more positive than in controls (Figure 5C and D; Table I), indicating a roughly two-fold increase in $[Cl^-]_i$ when neglecting the HCO_3^- conductance of $GABA_ARs$ (Kaila and Voipio, 1987). In PC-ΔKcc3 mice, E_{GABA} was undistinguishable from littermate controls (Figure 5D). Likely due to different genetic backgrounds, the shift in E_{GABA} (∼15 mV; Figure 5D) was smaller in double conditional KO (PC-Δ(Kcc2 + Kcc3)) than between PC-ΔKcc2 and their respective littermates. The resting membrane voltage (*V*) of PCs was not affected by disrupting *Kcc2* or *Kcc3* (Figure 5D; Table I). Hence Kcc2, but not Kcc3, plays a major role in setting resting $[Cl^-]_i$ of PCs.

The transport capacity of Cl^- extruders is not directly reflected in steady-state $[Cl^-]_i$. To investigate whether a contribution of Kcc3 becomes apparent in assays for net Cl^- transport, we examined Cl^- extrusion of PCs during and after Cl^- loading (Jin *et al*, 2005; Zhu *et al*, 2005). Depolarizing pulses were used to drive Cl^- into PCs through muscimol-activated $GABA_A$Rs (Figure 5E). Starting from different resting values (Figure 5D; Table I), $[Cl^-]_i$ increased rapidly during the loading phase (Figure 5F). In control mice, $[Cl^-]_i$ quickly reached steady state and then slightly decreased, possibly owing to an activation of Cl^- extruders (Figure 5F). By contrast, $[Cl^-]_i$ continued to increase slowly

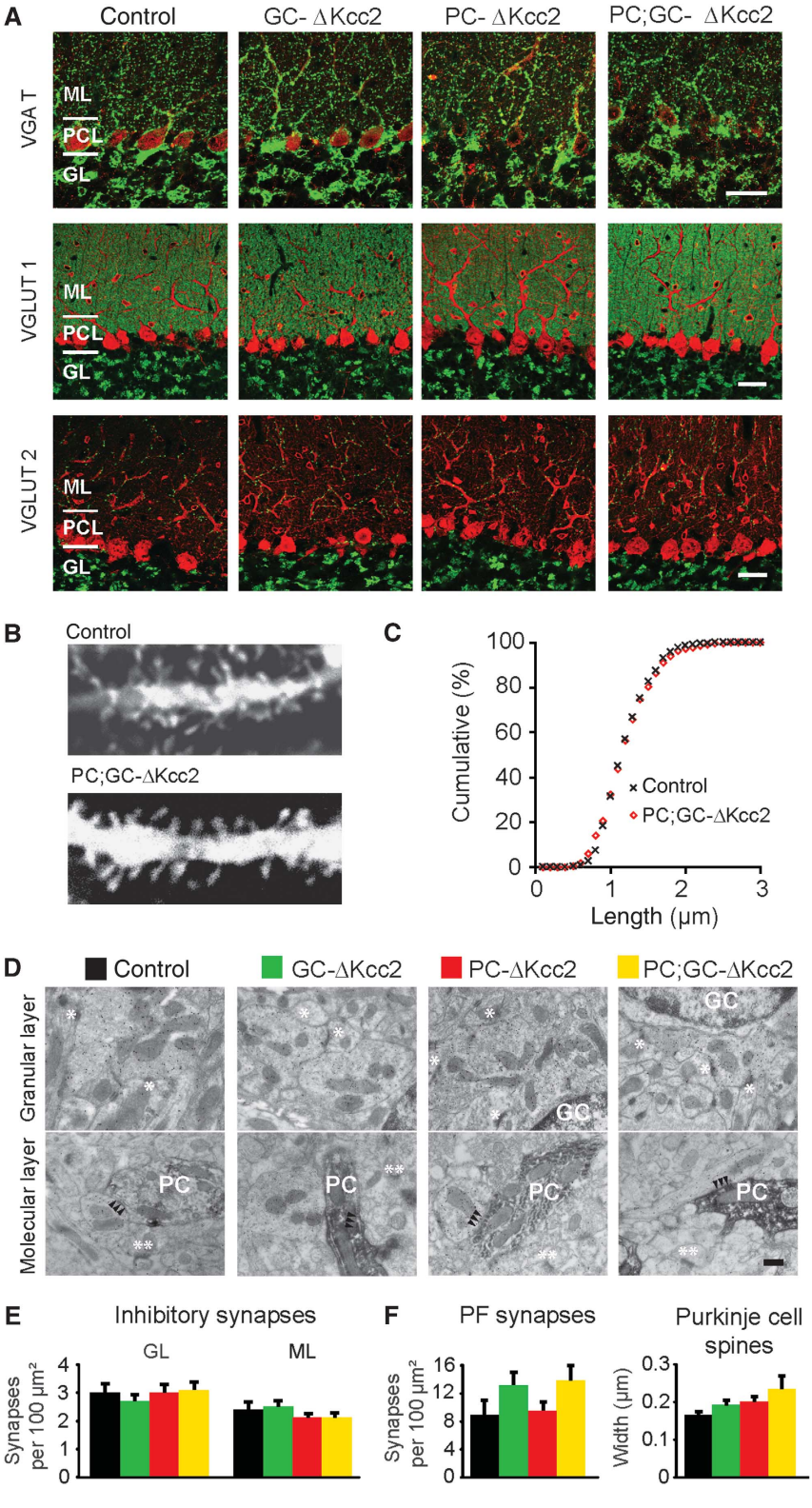

in PCs lacking Kcc2 or both Kcc2 and Kcc3. At the end of a 1-min muscimol washout period, control PCs had already recovered their resting $[Cl^-]_i$, whereas PCs of either PC-ΔKcc2 or PC-Δ(Kcc2 + Kcc3) mice similarly needed ~4 min to reach their initial $[Cl^-]_i$. In *Kcc3*$^{-/-}$ PCs, recovery of resting $[Cl^-]_i$ was as fast as in control PCs (Supplementary Figure S2). Thus, also this test failed to detect a contribution of Kcc3 to Cl^- regulation, both in the absence and presence of Kcc2.

Kcc2-mediated Cl^- extrusion contributes to the resting membrane potential in GCs

Whereas E_{GABA} of PCs could be obtained by perforated patch voltage-clamp measurements, this approach is problematic with the small GCs due to high access resistance of the smaller patch pipettes needed for these cells (Brickley *et al*, 1996). We instead resorted to cell-attached recordings of $GABA_AR$ currents (Tyzio *et al*, 2006) and voltage-gated K^+ currents (Fricker *et al*, 1999) to determine the driving force for Cl^- in the presence of GABA (DF_{GABA}) and the membrane voltage *V*, respectively (Figure 6). As Kcc3 was not detected in GCs (Figure 2C), we only analysed *Kcc2*$^{lox/lox}$ and GC-ΔKcc2 mice.

$GABA_AR$ single-channel activity was detected in ~80% of patches from control or GC-ΔKcc2 GCs (Figure 6A). They were blocked when $GABA_AR$ blocker gabazine was included in the pipette (Supplementary Figure S3A and B). DF_{GABA} was determined as the potential where single-channel currents reversed polarity. The slightly depolarizing action of GABA (~7 mV) agrees well with the one (~8 mV) reported for rat GCs (Brickley *et al*, 1996) and was confirmed in perforated patch measurements under current clamp (Supplementary Figure S4A). Surprisingly, it was not affected by the absence of Kcc2 (Figure 6A; Table I).

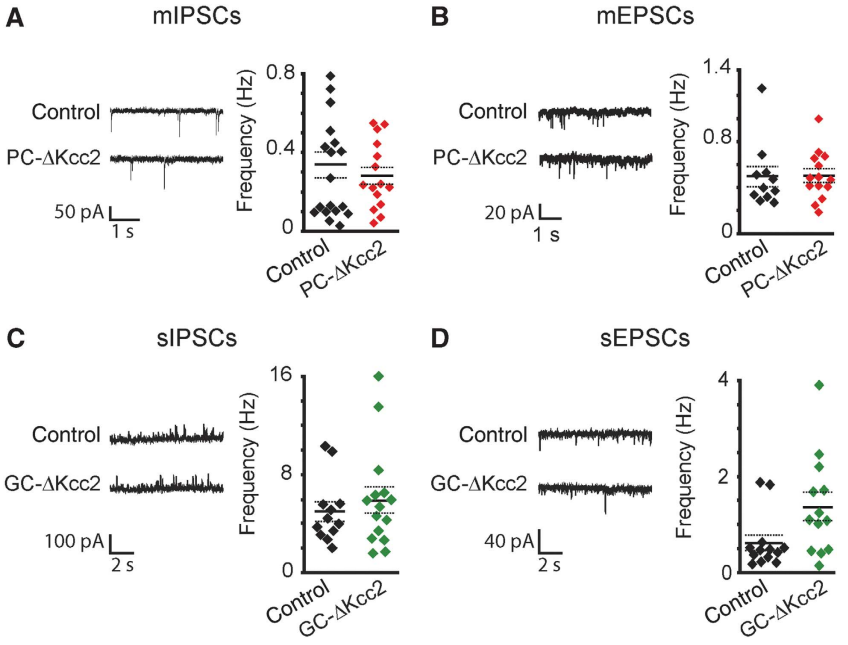

Figure 4 Frequency of miniature and spontaneous excitatory and inhibitory postsynaptic currents in Purkinje cells. (**A**) The frequency of mIPSCs recorded from PCs in the presence of tetrodotoxin is not changed by PC-specific *Kcc2* disruption, nor (**B**) is there a change in the frequency of mEPSCs. The amplitudes of mEPSCs (control: 15.2 ± 1.1 pA, $n = 11$ cells and PC-ΔKcc2: 14.7 ± 0.8 pA, $n = 14$ cells) and mIPSCs (control: 50 ± 5.8 pA, $n = 19$ cells and PC-ΔKcc2: 62 ± 5.3 pA, $n = 15$ cells) were not changed. (**C**) Spontaneous IPSCs and (**D**) EPSCs of PCs measured without tetrodotoxin. Each panel shows representative traces (left) and diagrams (right) that display individual data points, with mean values ± s.e.m. indicated by solid and dashed lines. Control, *Kcc2*$^{lox/lox}$ mice (P25–34).

Figure 3 Inhibitory and excitatory synapses appear unchanged upon cell-specific *Kcc2* deletion. (**A**) Confocal sections of cerebellar cortex from adult mice stained against VGAT (vesicular GABA transporter, green), VGLUT1 or VGLUT2 (vesicular glutamate transporter 1 and 2, green) as marker for inhibitory or excitatory synapses reveal no differences between the genotypes. Co-staining against parvalbumin is shown in red (ML, PCL, and GL, molecular layer, Purkinje cell layer, and granule cell layer, respectively). Scale bars: 40 μm. (**B**) Biocytin filling of PCs from adult *Kcc2*$^{lox/lox}$ (control) (above) and PC;GC-ΔKcc2 mice (below) reveals no obvious difference in spine number and morphology. (**C**) Cumulative distribution of PC dendritic spine lengths from control and PC;GC-ΔKcc2 mice. (**D**) Electron micrographs of the granular layer (top panels) and molecular layer (bottom panels) of control mice, GC-ΔKcc2, PC-ΔKcc2, and PC;GC-ΔKcc2 mice (from left to right). Arrowheads indicate symmetric synapses. Asterisks indicate synapses in glomeruli (granular layer) and asymmetric synapses in the molecular layer. Scale bar: 500 nm. (**E**) The density of inhibitory synapses in granular layer glomeruli of GC-ΔKcc2 mice ($n = 4$) was indistinguishable from controls ($n = 4$), as is that in PC-ΔKcc2 ($n = 4$) and PC;GC-ΔKcc2 mice ($n = 4$) ($P = 0.89$, 1.0, and 0.99, respectively; one-way ANOVA). The density of inhibitory and excitatory synapses onto Purkinje cells in GC-ΔKcc2, PC-ΔKcc2, and PC;GC-ΔKcc2 mice neither differed from controls ($P = 0.97$, 0.75, and 0.72, respectively; one-way ANOVA). (**F**) The density of parallel fiber (PF) synapses onto Purkinje cell spines in control mice was indistinguishable from that in GC-ΔKcc2, PC-ΔKcc2, and PC;GC-ΔKcc2 mice ($P = 0.26$, 0.99, and 0.18, respectively; one-way ANOVA). Similarly, the width of Purkinje cell spine necks did not differ between controls, GC-ΔKcc2, PC-ΔKcc2, and PC;GC-ΔKcc2 mice ($P = 0.82$, 0.61, and 0.09, respectively; one-way ANOVA). Colour codes as indicated on top of panels in (**D**). Error bars, s.e.m.

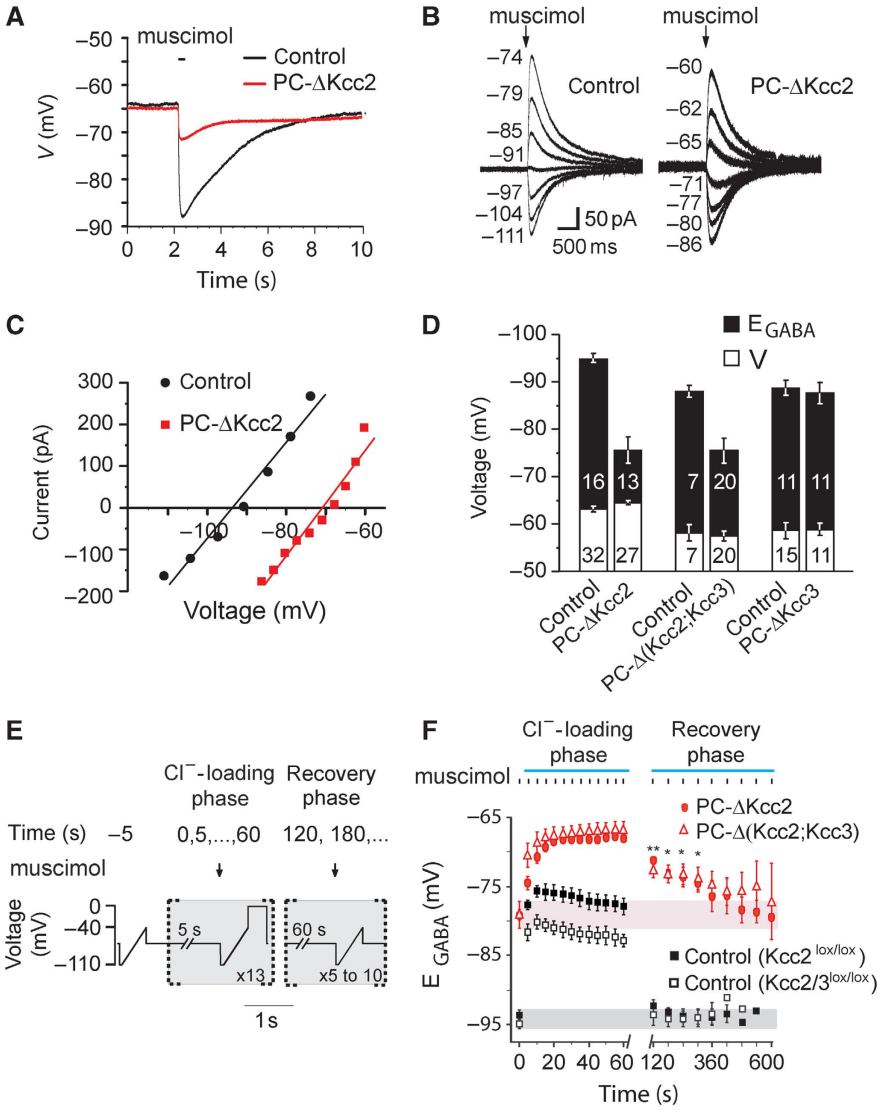

Figure 5 Role of Kcc2 and Kcc3 in setting $[Cl^-]_i$ of Purkinje cells. (**A**) Effect of the $GABA_AR$ agonist muscimol on PC membrane voltage *V* from control and PC-ΔKcc2 mice. (**B**) Currents elicited by puff application of muscimol to PCs of $Kcc2^{lox/lox}$ (control) and PC-ΔKcc2 mice held at different potentials (indicated left from traces; series resistance corrected) in the perforated patch configuration. (**C**) Determination of E_{GABA}. Maximum current after muscimol application plotted against voltage. The intersection of the fitted line with $I=0$ gives E_{GABA}. (**D**) Summary of *V* and E_{GABA}. 'Floxed' animals served as paired controls (number of cells indicated on bars). (**E**) Protocol to determine Cl^- extrusion following intraneuronal Cl^- loading. A series of voltage ramps (500 ms, from −110 to −40 mV) combined with a 50-ms application of 50 μM muscimol (arrows) was used to determine changes in E_{GABA} during the loading phase (for 60 s, puff application and voltage ramps at 0.2 Hz, each ramp followed by a 400-ms step to 0 mV) and the recovery phase (one muscimol puff/minute). The first voltage ramp ($t=-5$ s) was not combined with muscimol application. Analysis of the recovery phase started 60 s after the loading phase ($t=120$ s). (**F**) Time course of E_{GABA} during and after Cl^--loading phase for PC-ΔKcc2 mice ($n=7$) and control littermates ($n=5$), and PC-Δ(Kcc2 + Kcc3) mice ($n=6$) and control littermates ($n=5$). Coloured background displays initial E_{GABA} of each genotype and asterisks significant differences between PC-ΔKcc2 and control mice. Plots display averages ± s.e.m. Age of mice: P25–P65.

Table I Effect of Kcc2 deletion on resting membrane potential *V*, E_{GABA}, driving force for GABAergic currents (DF_{GABA}) and estimated intracellular Cl^- concentration ($[Cl^-]_i$) in granule and Purkinje cells

	Granule cell			Purkinje cell		
	$Kcc2^{+/+}$	$Kcc2^{-/-}$	Δ	$Kcc2^{+/+}$	$Kcc2^{-/-}$	Δ
V (mV)	−86.3 ± 2.2 (22)	−71.3 ± 1.9 (39)	15.0 ± 2.9	−63.1 ± 0.6 (32)	−64.5 ± 0.5 (27)	−1.4 ± 0.8
E_{GABA} (mV)	−79.1 ± 2.3	−64.3 ± 1.9	14.5 ± 3.2	−94 ± 1 (16)	−75 ± 3 (13)	19 ± 3.2
DF_{GABA} (mV)	7.2 ± 0.6 (11)	7.0 ± 0.3 (15)	−0.2 ± 1.2	−30.9 ± 1.2	−10.5 ± 1.1	20.4 ± 1.6
Estimated $[Cl^-]_i$ (mM)	5.6 ± 1.0	10.1 ± 1.5	4.5 ± 1.8	3.2 ± 0.1	6.6 ± 1	3.4 ± 1

$[Cl^-]_i$ was estimated from E_{GABA} and $[Cl^-]_o$ using the Nernst equation, but neglecting the HCO_3^- permeability of GABA receptors. These values are therefore given as estimates. Values represent arithmetic means ± s.e.m., with number of measurements given in brackets. Δ, Difference between respective values of $Kcc2^{+/+}$ (control) and $Kcc2^{-/-}$ mice. Age of mice: P25–65 (PCs) and P30–62 (GCs).

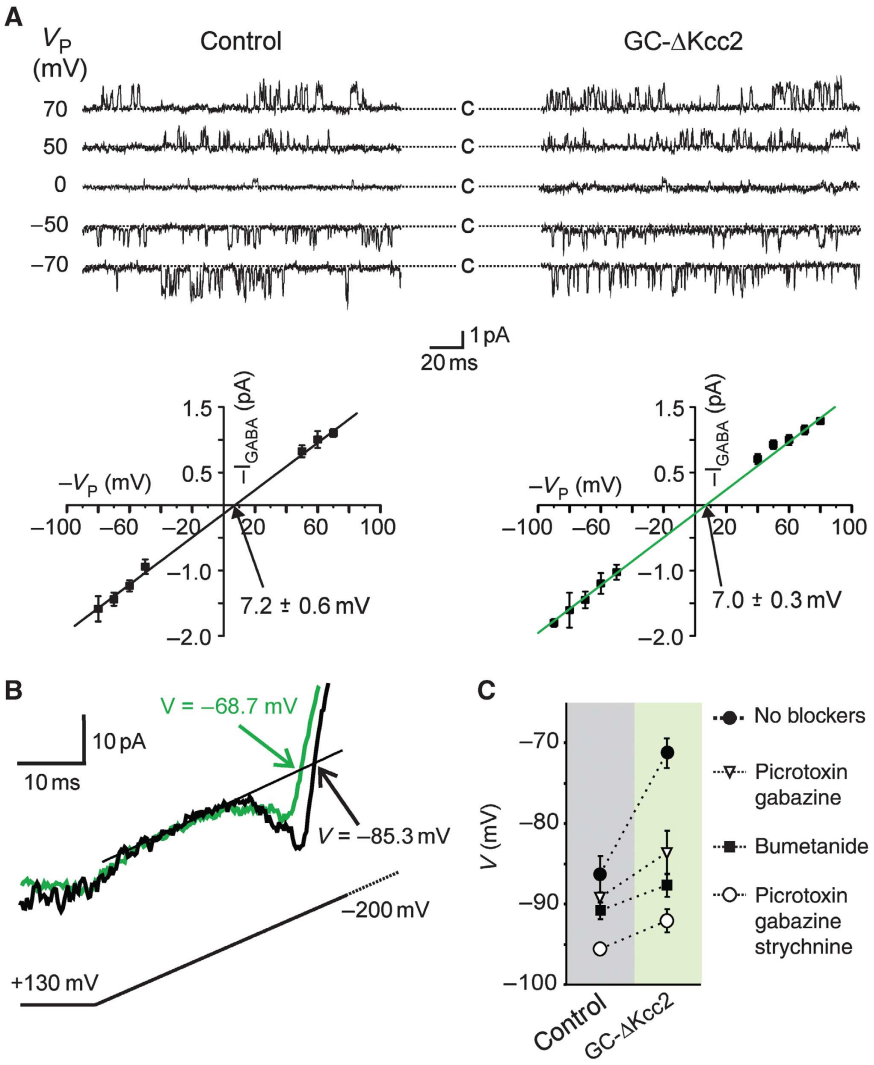

Figure 6 *Kcc2* deletion in granule cells alters resting *V*, but not the Cl^- driving force (DF_{GABA}). (**A**) Cl^- driving force determined by currents through $GABA_A$ receptors in cell-attached recordings. *Top*: single-channel recordings at different pipette voltages from *Kcc2*$^{lox/lox}$ (control) and GC-ΔKcc2 GCs. 'c', closed state. *Below*: mean single-channel currents as function of *V*. Linear regression (line) shows that *Kcc2* deletion does not change the Cl^- driving force (arrow). Single-channel conductance and mean open time were similar for both genotypes (18.4 ± 0.3 and 18.3 ± 0.4 pS, and 0.40 ± 0.02 and 0.41 ± 0.02 ms for control and GC-ΔKcc2, respectively). (**B**) *V* determined from K_V channel currents measured in cell-attached mode measured from other GCs of the same cerebellar region. Typical recordings for a GC-ΔKcc2 (green) and control (black) GC. The intersection of a linear fit to the linear ('leak') current (from ∼ +70 to +20 mV) with recorded outward currents gives *V*. *Below*: voltage protocol. (**C**) *V* of GCs from GC-ΔKcc2 mice and control littermates in the absence or presence of blockers for $GABA_A$Rs (picrotoxin and gabazine, 100 μM each), $GABA_A$Rs + GlyRs (additionally 1 μM strychnine), and Nkcc1 (10 μM bumetanide). Data are mean ± s.e.m. Number of experiments: 'no blockers' ($n = 22$, control; $n = 39$, GC-ΔKcc2), picrotoxin + gabazine ($n = 12$, control; $n = 19$, GC-ΔKcc2), picrotoxin + gabazine + strychnine ($n = 9$, control; $n = 11$, GC-ΔKcc2), and bumetanide ($n = 26$, control; $n = 27$, GC-ΔKcc2). Age of mice: P30–P62.

To determine the resting *V*, voltage ramps from +130 to −200 mV were applied to cell-attached GC patches (Fricker *et al*, 1999). The reversal potentials of elicited K_v currents correspond to *V* as the K^+ concentration of the pipette solution (155 mM) mimics intracellular [K^+] (Fricker *et al*, 1999; Figure 6B). *Kcc2* disruption depolarized GCs by ∼15 mV (Table I). These values were confirmed by perforated patch current-clamp measurements (Supplementary Figure S5). From these values and $E_{GABA} = DF_{GABA} + V$, we deduce that $[Cl^-]_i$ of GCs increased about two-fold upon *Kcc2* disruption (Table I).

The finding that *V* closely followed changes in E_{GABA} indicated that GCs display a sizeable Cl^- conductance at rest. As GCs are tonically inhibited by ambient GABA (Brickley *et al*, 2001), we blocked $GABA_A$R Cl^- channels with gabazine and picrotoxin. This did not significantly change *V* of control GCs, but cells lacking Kcc2 were hyperpolarized to voltages similarly to those of controls (Figure 6C). With conjoint blockage of GlyRs and $GABA_A$Rs, GCs of both control and GC-ΔKcc2 mice were hyperpolarized to $V = -95.6 \pm 2$ mV and $V = -92.1 \pm 4.9$ mV, respectively (Figure 6C). Thus, both $GABA_A$Rs and GlyRs influence the resting potential of GCs.

These results, together with the value of E_{GABA}, which was slightly positive to *V* (Table I), indicated a depolarizing Cl^- efflux in GCs. Even control cells hyperpolarized when both receptors were blocked, indicating that $[Cl^-]_i$ is above equilibrium even in the presence of Kcc2—a result agreeing with the depolarizing effect of applied GABA. As the Cl^--loader *Nkcc1* is robustly expressed in GCs (Supplementary Figure

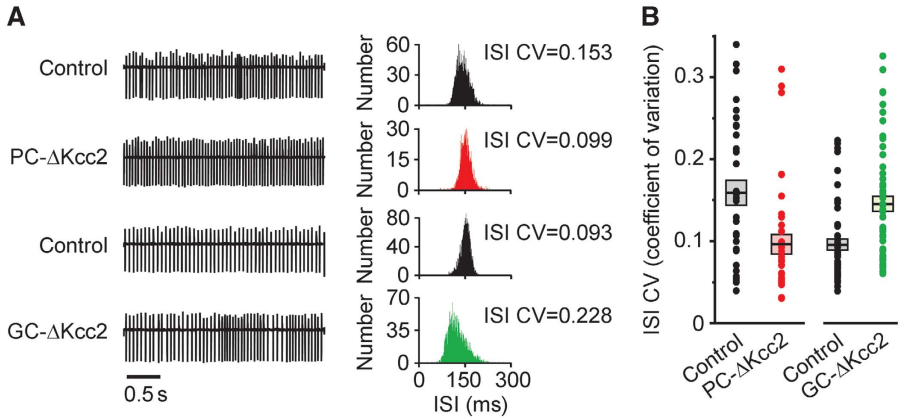

Figure 7 Spontaneous spiking of Purkinje cells in sagittal cerebellar slices of adult (11–21-week-old) mice. (**A**) Representative traces (left) and ISI histograms (right) of PCs recorded at room temperature in the absence of inhibitors in loose cell-attached patches from PC-ΔKcc2 mice and control littermates (upper traces) and GC-ΔKcc2 mice and control littermates (lower traces). (**B**) The coefficient of variation of interspike interval (CV) for PC-ΔKcc2 mice ($n=36$, average frequency: 21.6 ± 2 Hz), GC-ΔKcc2 mice ($n=55$, 14.4 ± 1 Hz) and their respective control littermates ($n=33$, 16.6 ± 2 Hz and $n=50$, 12.7 ± 1 Hz). The plot shows averages (black horizontal lines) ± s.e.m. (Boxes) (ISI CV = 0.159 ± 0.015 and 0.097 ± 0.012 for control and PC-ΔKcc2 mice, respectively; $P<0.05$, *t*-test) (ISI CV = 0.096 ± 0.007 and 0.145 ± 0.009 for control and GC-ΔKcc2 mice, respectively; $P<0.0001$). Individual measurements are shown as circles. Most likely differences in genetic background underlie the difference between control ISI CVs.

S6), we blocked this transporter with 10 μM bumetanide. At this concentration, bumetanide has no effect on $GABA_A$Rs of GCs (Korpi *et al*, 1995; Hamann *et al*, 2002). Bumetanide hyperpolarized GC-ΔKcc2 GCs to close control values (Figure 6C; Supplementary Figure S4A) and strongly reduced muscimol-induced depolarizations in GCs of both GC-ΔKcc2 and control mice (Supplementary Figure S4A). In GC-ΔKcc2 mice, Nkcc1-driven intracellular Cl^- accumulation is not counterbalanced by the Cl^- extruder Kcc2. Therefore, we expect a higher intracellular Cl^- concentration that should increase the chemical gradient for Cl^- efflux, resulting in larger depolarizing Cl^- currents through tonically active GABA and glycine receptors. Indeed, pharmacological blockade of these receptors hyperpolarized GC-ΔKcc2 GCs more than control cells (Figure 6C). K2P K^+ channels, which are highly expressed in GCs and are responsible for their rather negative *V* (Duprat *et al*, 1997; Karschin *et al*, 2001; Aller *et al*, 2005), may mediate this hyperpolarization.

In conclusion, the deletion of *Kcc2* in GCs does not change their slightly depolarizing GABA response that may lead to a shunting inhibition in either genotype. However, the depolarization of $Kcc2^{-/-}$ GCs indicates that they may be more excitable than control GCs, agreeing with the higher frequency of sEPSCs in PCs of GC-ΔKcc2 mice (Figure 4D). While muscimol by itself induced action potentials neither in WT nor in GC-ΔKcc2 GCs (Supplementary Figure S4A), we needed to inject less depolarizing current into $Kcc2^{-/-}$ GCs to elicit action potentials (Supplementary Figure S4B).

Spontaneous spiking of PCs

To investigate whether the disruption of Kcc2 in GCs or PCs affects the electrical output of the cerebellar cortex, we investigated the spontaneous firing of PCs in slice preparations. The frequency of firing was similar between PCs from PC-ΔKcc2, GC-ΔKcc2, and corresponding control littermate mice (Figure 7). However, the regularity of PC firing, measured as the coefficient of variation of the interspike interval (ISI CV), was significantly reduced in PC-ΔKcc2 mice, indicating a higher firing regularity (Figure 7A and B). By contrast, and in line with an increased excitability of GCs (Wulff *et al*, 2009), spontaneous firing of PCs from GC-ΔKcc2 mice was more irregular compared with control littermates (Figure 7B).

Effect of GC- and/or PC-specific Kcc2 deletion on learning and consolidation

None of the mutants showed any overt sign of motor deficits. To assess cerebellar motor performance, we tested compensatory eye movements in GC-ΔKcc2, PC-ΔKcc2, and PC;GC-ΔKcc2 mice in comparison with their control littermates. GC-ΔKcc2 mice did not show any significant deficit in the gain (amplitude) or phase (timing) of their optokinetic reflex (OKR), vestibulo-ocular reflex (VOR) in the dark, or vestibulo-ocular reflex in the light (visual VOR or VVOR) (Figure 8A–C). In contrast, both the PC-ΔKcc2 and PC;GC-ΔKcc2 mice showed a small, but significant, decrease in the gain of their OKR compared with controls (Figure 8A), while PC;GC-ΔKcc2 mice also revealed a significant phase lag during OKR, VOR as well as VVOR (Figure 8A–C).

Next, we investigated the impact of Kcc2 ablation in GCs on short-term and long-term motor learning and consolidation, by subjecting the mice to VOR adaptation paradigms. Short-term learning was induced by providing mismatch vestibular and visual stimulation during five 10-min sessions with in-phase table and drum rotation (both 5° amplitude at 0.6 Hz), effectively inducing a decrease of the VOR gain. GC-ΔKcc2 mice did not show any deficit during this short-term, gain-decrease learning (Figure 8D). In contrast, PC-ΔKcc2 and PC;GC-ΔKcc2 mice showed a significant impairment in VOR decrease learning compared with controls (Figure 8D), that appeared not to be related to the L7/pcp2-promotor induced retinal Cre expression (Supplementary Figure S7). When we measured the VOR the next day after keeping the animals overnight in the dark, gain consolidation in GC-ΔKcc2 mice was comparable to that of controls (Figure 8E, left panel). Here too, PC-ΔKcc2 and PC;

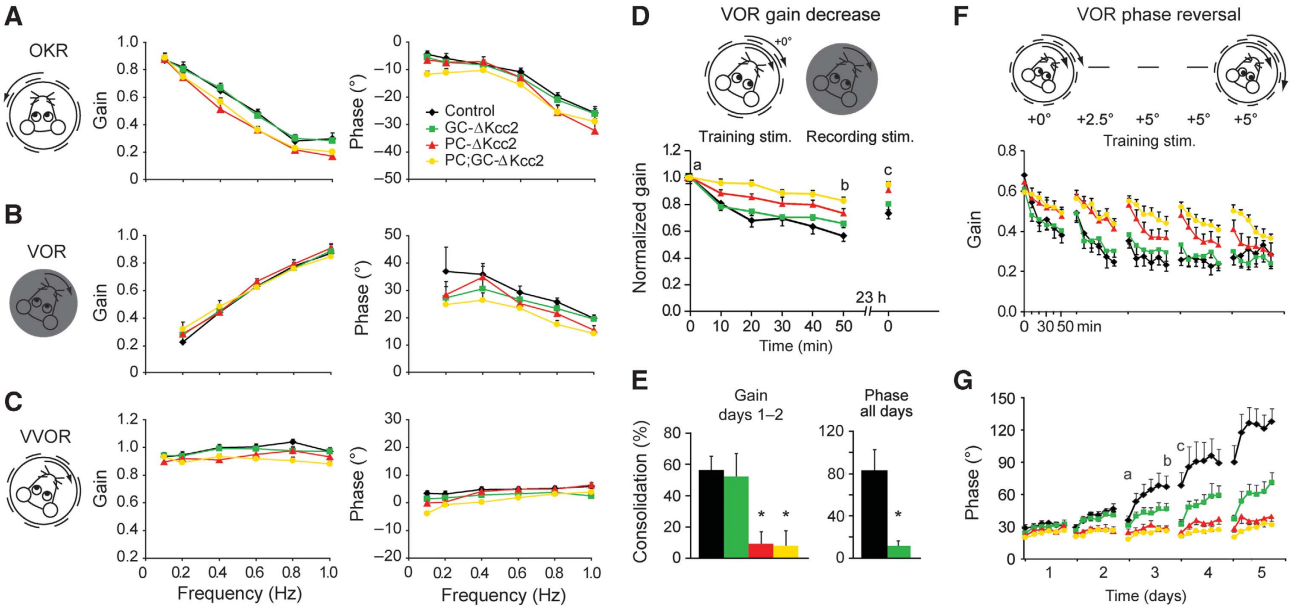

Figure 8 Motor performance (**A**–**C**), learning and consolidation (**D**–**G**) in Kcc2 mutant mice. (**A**–**C**) Compensatory eye movements in adult control ($n=8$), GC-ΔKcc2 ($n=8$), PC-ΔKcc2 ($n=8$), and PC;GC-ΔKcc2 ($n=10$) mice. Mice were subjected to visual (OKR) and/or vestibular stimulation (in dark, VOR; in light, VVOR) and gain (ratio of eye to stimulus velocity) and phase (difference in degrees between eye and stimulus) were calculated. (**A**) OKR gain was not affected in GC-ΔKcc2 mice ($P=1.00$), but was significantly lower in PC-ΔKcc2 and PC;GC-ΔKcc2 mice than in controls ($P=0.015$ and 0.035, respectively). (**B**) VOR gain values did not differ between Kcc2 conditional KO and control mice (all $P>0.9$). (**C**) VVOR gain values did not differ among Kcc2 mutants and control mice ($P=0.716$, 0.369, and 0.074 for GC-ΔKcc2, PC-ΔKcc2, and PC;GC-ΔKcc2 mice versus controls). PC;GC-ΔKcc2 mice revealed a significant phase lag in OKR ($P=0.002$), VOR ($P=0.006$), and VVOR ($P=0.001$), whereas the other mutants did not (all $P>0.14$ and >0.24 for GC-ΔKcc2 and PC-ΔKcc2 mice, respectively). (**D**) Short-term VOR gain-decrease learning was not impaired in GC-ΔKcc2 ($n=10$) compared with control ($n=9$) mice ($P=0.74$; repeated measures ANOVA), whereas PC-ΔKcc2 ($n=10$) and PC;GC-ΔKcc2 ($n=10$) mice showed a significant impairment ($P<0.005$ and 0.001, respectively). (**E**) Likewise, gain consolidation (calculated as $100\% \cdot (a-c)/(a-b)$) overnight was not affected in GC-ΔKcc2 mice ($P=0.99$ versus controls; one-way ANOVA), whereas PC-ΔKcc2 and PC;GC-ΔKcc2 showed a significant deficit in gain consolidation ($P=0.030$ and 0.025, respectively). (**F**, **G**) VOR phase reversal training induced a significant phase change in GC-ΔKcc2 mice during each consecutive day ($P<0.005$ for days 2–5, paired Student's *t*-test). However, from day 4 onwards their VOR phase reversal was impaired compared with controls ($P=0.015$ and <0.001 on days 4 and 5). This difference is the result of the inability of GC-ΔKcc2 mice to consolidate their phase learning overnight (right panel in (**E**); $P=0.007$; Student's *t*-test). Due to their deficits in VOR gain learning and consolidation, PC-ΔKcc2 and PC;GC-ΔKcc2 mice were also unable to reverse their VOR phase ($P<0.001$ on day 5 for both mutants versus controls). Error bars denote s.e.m., all *P*-values are based on repeated measures ANOVA unless stated otherwise.

GC-ΔKcc2 mice showed a significant deficit, suggesting that inhibition provided by the molecular layer interneurons rather than the excitability of GCs contributes to gain consolidation (Wulff *et al*, 2009).

Finally, we subjected the mice to a long-term VOR phase reversal training paradigm, which allows the identification of deficits in the adaptation of timing of movements (Wulff *et al*, 2009). In this paradigm, the mice are subjected, after the first day of gain-decrease training, to in-phase table (5° at 0.6 Hz) and drum stimulation with drum amplitude increasing to 7.5° on day 2 and 10° on days 3–5 (all at 0.6 Hz), effectively causing a reversal of the VOR phase (Figure 8F and G). Although GC-ΔKcc2 mice were able to significantly modify their VOR phase on each training day, their VOR phase adjustment was impaired compared with controls from day 4 onwards. The explanation for this observation can be found in the fact that the GC-ΔKcc2 mice, in contrast to controls, were not able to consolidate their phase learning overnight ($P=0.007$; Student's *t*-test) (Figure 8E, *right panel*; Figure 8G). PC-ΔKcc2 and PC;GC-ΔKcc2 mice were, in line with their deficits in VOR gain learning and consolidation, unable to reverse the phase of their eye movements. Together, these data indicate that the control of excitability of GCs contributes to phase learning and is necessary for its consolidation.

Discussion

We investigated the role of GABAergic inhibition in cerebellar function by selectively altering the Cl^- gradient across membranes of GCs and PCs. A rise in $[Cl^-]_i$, as observed with disruption of the Cl^--extruding K-Cl cotransporter Kcc2, is expected to decrease the inhibition by GABA. This was indeed observed when *Kcc2* was disrupted in PCs, but not in GCs, whose resting *V* depended on Cl^-. Different sets of aspects of cerebellar learning were affected when increasing $[Cl^-]_i$ in GCs or PCs. In spite of the presumed role of Kcc2 in neuronal development and morphogenesis, we observed no structural defects upon cell type-specific *Kcc2* deletion.

Kcc2 and neuronal development

In addition to affecting neuronal excitability by raising $[Cl^-]_i$, disruption of *Kcc2* might also have changed neuronal morphology. A depolarizing GABA response during early development is thought to be important for neuronal development (Ben-Ari, 2002). In most parts of the rodent CNS, the 'GABA switch' from depolarizing to hyperpolarizing $GABA_AR$ responses takes place during the first few weeks after birth. The switch is caused by a decrease of intraneuronal $[Cl^-]$ that changes the direction of Cl^- fluxes from outward to inward. During that period, glutamatergic synaptic transmission

occurs almost exclusively through NMDA receptors that need a depolarization to be relieved from their Mg^{2+} block. The depolarizing GABA response during early development is thought to provide this initial depolarization, with Ca^{2+} influx through NMDA receptors potentially impinging on neuronal gene transcription and development (Ben-Ari *et al*, 1997). Indeed, premature lowering of intraneuronal $[Cl^-]$ in tectal neurons of *Xenopus* by Kcc2 expression blocks their AMPA-R mediated retinotectal transmission (Akerman and Cline, 2006), and premature expression of Kcc2 in rat ventricular progenitors and cortical neurons impaired morphological maturation (Cancedda *et al*, 2007). Global disruption of the Cl^--loader Nkcc1, which also decreases GABAergic excitation, drastically reduces the maturation of glutamatergic and GABAergic transmission in the hippocampal CA1 region without affecting brain morphology (Pfeffer *et al*, 2009).

Kcc2 disruption, by contrast, would increase rather than decrease the extent of GABAergic excitation, and would prolong or perpetuate the period during which it is observed. The perinatal lethality of $Kcc2^{-/-}$ mice (Hübner *et al*, 2001b) precludes an analysis at time points when Kcc2 reaches its adult expression levels in the WT. Our present data now show that reduced GABAergic inhibition of PCs has no detectable effect on their morphology.

On the other hand, Kcc2 was described as a key factor in the maturation of dendritic spines independent of its ion transport function (Li *et al*, 2007). The C-terminus of Kcc2 was shown to interact with the cytoskeleton-associated protein 4.1N. In cultures of cortical neurons, and to a lesser extent in brain from mice estimated to express only 17% of WT Kcc2 levels, drastic changes in (glutamatergic) spine morphology and a significant reduction in the number of functional synapses were observed (Li *et al*, 2007). The latter observation was confirmed by an ~2-fold reduction in mEPSC frequency (Li *et al*, 2007). By contrast, we observed changes neither in synapse number, spine morphology, nor in the frequency of mEPSCs and mIPSCs of PCs lacking Kcc2. It remains to be determined whether the effects of Kcc2 described by Li *et al* (2007) is cell type specific, can only be observed in cell culture but not *in vivo*, or whether this effect is suppressed when Kcc2 is deleted from only a sub-population of neurons, as in the present mouse models. Another difference to the study of Li *et al* (2007) is the fact that in our work *Kcc2* was disrupted by Cre-mediated exon excision during the first weeks after birth. Interestingly, when Kcc2 was knocked down by siRNA in neurons after 14 days in culture, only subtle changes in spine morphology were observed (Gauvain *et al*, 2011). By contrast, the number of synapses was changed in constitutive $Kcc2^{-/-}$ mice already at embryonic stages (Khalilov *et al*, 2011). Hence, the onset of Kcc2 deletion may determine its influence on the number and morphology of synapses. In any case, our detailed morphological analysis excludes morphological effects as an explanation for the observed (patho-)physiological effects of *Kcc2* deletion.

Intracellular Cl^- homeostasis in cerebellar PCs and GCs

The cytoplasmic Cl^- concentration is of particular importance for neurons, since it determines their response to GABA and glycine. In immature neurons, $[Cl^-]_i$ is above electrochemical equilibrium and accordingly opening of $GABA_A$Rs or GlyRs entails a depolarizing Cl^- efflux that may even be excitatory (Cherubini *et al*, 1991) and which is believed to be important for brain development (Ben-Ari *et al*, 1997; Ben-Ari, 2002). Upon maturation, most CNS neurons develop an inhibitory response to GABA, because the increased expression (Stein *et al*, 2004; Ludwig *et al*, 2011) or activation (Tyzio *et al*, 2006; Rinehart *et al*, 2009) of Cl^- extruding transporters lower their $[Cl^-]_i$. There is consensus that the K-Cl cotransporter Kcc2 is the main Cl^- extruder of neurons (Rivera *et al*, 1999; Hübner *et al*, 2001b). Our work establishes Kcc2 as the main Cl^- extruder for PCs and GCs.

Unexpectedly, the GABA response of PCs lacking Kcc2 remained slightly hyperpolarizing, implying that their $[Cl^-]_i$ stayed below electrochemical equilibrium. Other transporters which are potentially able to extrude Cl^- include Kcc3 and Na^+-coupled Cl^-/HCO_3^- exchangers that exploit the Na^+ gradient for extruding Cl^- against its gradient. The prime candidate was Kcc3, as it is robustly expressed in PCs (Boettger *et al*, 2003). Although previous work showed that the constitutive disruption of *Kcc3* lowers $[Cl^-]_i$ in PCs at P12–P14, the main role of Kcc3 in neurons may be cell volume regulation (Boettger *et al*, 2003). Using mice older than P25, we found no significant effect of Kcc3 on $[Cl^-]_i$ of PCs even when they lacked Kcc2. Hence, the identity of the other putative Cl^- extruder of PCs remains unclear, but may be represented by the Na^+-coupled Cl^-/HCO_3^- exchanger SLC4A10 which is robustly expressed in PCs (Jacobs *et al*, 2008).

In contrast to PCs, GCs responded to GABA with a slight depolarization that may cause a shunting inhibition (Brickley *et al*, 1996). Depolarization by axonal $GABA_A$Rs was recently reported to be strong enough to increase GC excitability (Pugh and Jahr, 2011). Our data indicate that $[Cl^-]_i$ is slightly above electrochemical equilibrium also at GC cell bodies, although Kcc2 is active in these cells as revealed by the ~2-fold increase of $[Cl^-]_i$ upon *Kcc2* disruption. Even if GCs would express only Kcc2 and no Cl^- loader, the very negative resting potential of GCs (~−80 mV) will strongly reduce or even inverse the driving force for Cl^- exit, since the thermodynamic equilibrium of K-Cl cotransport is voltage independent. However, the effects of bumetanide and antagonists of $GABA_A$Rs and GlyRs showed that also the Cl^--loader Nkcc1 and a Cl^- conductance mediated by $GABA_A$Rs and GlyRs, respectively, contribute to GC Cl^- homeostasis. It may seem counterintuitive that Cl^- loaders and extruders are active in the same cell, but this situation is not unprecedented (Rust *et al*, 2006) and may serve to finely regulate $[Cl^-]_i$, the resting membrane potential and the electrical excitability of GCs in an active push-pull fashion.

Effects of Kcc2 disruption on cellular signal transduction

The disruption of *Kcc2* strongly reduced the GABA-induced hyperpolarization of PCs and should therefore decrease the strength of inhibitory synaptic input. The remaining small hyperpolarization, together with the increased membrane conductance, may suffice for a weak shunting inhibition of PCs. However, the ability of PCs to extrude Cl^- was strongly reduced in the absence of Kcc2, as revealed by our Cl^--loading experiments. Hence, in particular during repetitive GABAergic stimulation at PC dendrites, there may be a considerable increase of dendritic Cl^- that may further reduce synaptic inhibition. Thus, it is not surprising that the

impairments in vestibulo-ocular learning and consolidation are virtually identical to those observed with a PC-specific disruption of $GABA_A$Rs (Wulff *et al*, 2009).

The situation with GCs is more complex and more revealing. We were surprised to find that the electric response to GABA, a slight depolarization, was essentially the same when Kcc2 was lacking. Whereas this may suggest minimal effects on synaptic inhibition of GCs, we observed robust behavioural effects. This is probably a consequence of GC depolarization. In contrast to PCs, GCs express highly sensitive and non-inactivating $\alpha_6\delta$-containing $GABA_A$Rs (Laurie *et al*, 1992; Saxena and Macdonald, 1996; Brickley *et al*, 2001; Rossi *et al*, 2003; Hadley and Amin, 2007) and display tonic inhibition by ambient GABA (Brickley *et al*, 1996) which may come from their Golgi cell input (Brickley *et al*, 1996) or from glia (Lee *et al*, 2010). The constitutive depolarization upon *Kcc2* disruption renders GCs more excitable by lowering the threshold for depolarizing currents to elicit action potential firing, and possibly additionally by partially releasing the Mg^{2+} block of their NMDA receptors. Lowering the spiking threshold leads to potentiation of intrinsic excitability of GCs (Armano *et al*, 2000), and the NMDA receptors are implicated in the induction of presynaptic long-term potentiation at the mossy fibre to GC synapse (D'Angelo *et al*, 1999). Thus, it is likely that various forms of plasticity are affected in GC-ΔKcc2 mice, and that, as a consequence, their GCs produce additional spikes. Interestingly, a higher GC output can indeed be associated with an increase in irregularity of PC simple spike firing (Wulff *et al*, 2009) as observed in the current study.

Impact of cell-specific Kcc2 deletion on vestibulo-cerebellar function

We found that PC-specific deletion of Kcc2 decreased the efficacy of their inhibitory synaptic input and affected the ability to adjust and consolidate the gain and phase of the eye movements during visuovestibular mismatch training. These findings are in line with the VOR adaptation deficits that can be observed following PC-specific ablation of $GABA_A$Rs (Wulff *et al*, 2009). In contrast, the Kcc2 deletion from GCs resulted in a selective, but profound disruption of long-term, overnight phase consolidation, while both the gain and phase of the optokinetic and vestibular responses remained intact. Notably, mice with impaired induction of long-term potentiation at the mossy fibre to GC synapse displayed a similar deficit in the consolidation of VOR phase reversal (Andreescu *et al*, 2011). We also found that the PC;GC-ΔKcc2 mutants were the most affected group in that both their baseline motor performance and motor learning were severely compromised. This is probably due to the cumulative effect of decreasing the inhibitory synaptic input to PCs, while increasing the excitatory parallel fibre activation at the same time.

Impact of GC-specific Kcc2 deletion on PC output

Inhibition from molecular layer interneurons onto PCs has little impact on simple spike firing frequency. Instead, both chemical blockade (Hausser and Clark, 1997) and genetic (Wulff *et al*, 2009) disruption of $GABA_A$Rs predominantly affect the regularity of firing. Here, we used an alternative mechanism to eliminate the hyperpolarizing effect of GABAergic stimulation, by altering the Cl^- gradient across the membrane. In line with previous results (Wulff *et al*, 2009), PCs showed an increase in regularity, indicating that Cl^- is the main contributor to the GABAergic control of PC regularity. Notably, the deletion of *Kcc2* in cerebellar GCs had a reverse effect on PCs, causing them to fire more irregularly. We hypothesize that GCs, that are more excitable due to the lower action potential firing threshold, cause an increase in parallel fibre activity that enhances the frequency of both excitatory and inhibitory inputs to PCs. This corrupted input would then in turn lead to less regular firing (see model in Wulff *et al*, 2009). An increase in PC irregularity also occurs in the *tottering* mutant mice, which have a mutation in their voltage-gated P/Q-type calcium channels (Hoebeek *et al*, 2005). *Tottering* PCs have strong irregularities in their simple spike firing and large deficits in oculomotor control and baseline motor performance (Hoebeek *et al*, 2005; Stahl *et al*, 2006). By contrast, a mild increase in PC simple spike irregularity due to an increased excitability of GCs results in a more specific phenotype, in that particularly consolidation of the phase during reversal learning is affected.

A change in the regularity of PC simple spike firing may result from insufficient diversity of GC codings in the temporal domain. If this diversity is insufficient, climbing fibre driven plasticity imposed in the molecular layer cannot be used to efficiently select proper codings carried by the parallel fibres, simply because there may not be a sufficient number of proper parallel fibre codings generated in the granular layer that can be selected from De Zeeuw *et al* (2011).

In short, we conclude that Kcc2 cotransporters in cerebellar GCs serve to control their level of excitability, and that this level is critical to determine spatiotemporal patterning of simple spike activity in PCs, which in turn appears necessary for consolidation of phase learning. Importantly, and in contrast to the postulated morphogenic role of Kcc2 in neuronal development (Li *et al*, 2007), our study also shows that disruption of *Kcc2* has no effect on neuronal morphology and synapse formation *in vivo*.

Materials and methods

Mice

All animal experiments were approved by LaGeSo, Berlin, Germany or by the DEC, Utrecht, Netherlands. Generation of $Kcc2^{lox/lox}$ and $Kcc3^{lox/lox}$ mice followed standard procedures and is detailed in Supplementary Methods. $Kcc2^{lox/lox}$ and $Kcc3^{lox/lox}$ mice were crossed with L7/Pcp2::Cre mice (Barski *et al*, 2000) and Δα6::Cre mice (Aller *et al*, 2003) to delete *Kccs* in PCs and GCs, respectively. Animals were kept on a mixed genetic background and littermates were used as controls. Neither insertion of loxP sites, nor expression of Cre-recombinase itself had an impact on membrane voltage V or E_{GABA}.

Antibodies

The following antibodies were used: rabbit anti-Kcc2 (C-terminal peptide: KNEREREIQSITDESC), rabbit anti-Kcc3 (Boettger *et al*, 2003), mouse anti-VGAT guinea pig anti-VGLUT1, rabbit anti-VGLUT2 (all from Synaptic Systems), mouse anti-calbindin 28kd (Sigma), rabbit anti-calbindin D9k (Swant), and mouse anti-parvalbumin (Swant). Secondary antibodies were coupled to Alexa Fluor 488 or 555 (Molecular Probes). Nuclei were labelled using ToPro-3 (Molecular Probes).

Histology, immunohistochemistry, and biocytin labelling

In all, 50 μm sagittal floating sections from fixed cerebella (4% PFA) were cut using a sliding microtome (Microm, HM 430). Immunohistochemistry and histology were performed as described (Hübner *et al*, 2001b).

PCs were filled with biocytin by whole-cell patching with a pipette solution containing 10 mM biocytin and post-fixed in 4% PFA. Biocytin was visualized using Alexa 555-Streptavidin (Molecular Probes) using confocal microscopy. Dendritic spine length from shaft to the most distal part was quantified with the NeuronJ software.

Electron microscopy

Electron microscopy on ultrathin sections was done as described previously (De Zeeuw *et al*, 1989; Andreescu *et al*, 2007). For details, see Supplementary Methods.

In-situ hybridization

Sense and antisense digoxigenin-UTP-labelled riboprobes (DIG RNA labeling Mix, Roche) were generated with T7 or SP6 RNA polymerase (Roche), respectively, from a linearized Kcc3 mouse cDNA clone (bps 146–1056) or from an Nkcc1 cDNA (bps 2246–2761). *In-situ* hybridization on sagittal cryosections of mouse brains was performed as described (Braissant and Wahli, 1998).

Electrophysiology

Parasagittal slices (200 μm) from cerebella of P25 to 21-week-old mice were prepared using a vibratome (Leica). Gramicidin perforated patch recordings were essentially performed as described (Hübner *et al*, 2001a, b). V was determined with a MultiClamp 700B amplifier (Molecular Devices) in current-clamp mode with $I=0$. GABA reversal potential (E_{GABA}) of PCs was measured in voltage-clamp mode. For details, see Supplementary Methods.

Spontaneous firing of PCs was recorded in the absence of blockers in cell-attached mode using pipettes were filled with ACSF. mIPSC and mEPSC were measured on PCs in the whole-cell mode at −70 mV in the presence of 2 μM TTX and 10 μM gabazine (SR-95531; Sigma) (for mEPSCs) or 1 μM TTX, 50 μM D-AP5 and 10 μM CNQX (for mIPSCs). Pipette solution contained in mM: 135 CsCl, 10 HEPES, 0.2 EGTA, 2 ATP, 0.3 GTP, and 10 glucose.

sIPSCs and sEPSCs were measured on PCs in whole-cell mode at −75 mV (sEPSCs) and +20 mV (sIPSCs) in the absence of blockers in the extracellular solution. Pipette solution consisted of (in mM) 130 Cs-methanesulphonate, 7 NaCl, 2 Mg-ATP, and 10 HEPES pH 7.3.

Single-channel recordings of $GABA_A$Rs of GCs (age of mice: 4–8 weeks) were performed in the cell-attached configuration, with a pipette solution (in mM): 120 NaCl, 5 KCl, 0.1 $CaCl_2$, 10 $MgCl_2$, 20 TEA-Cl, 5 4-AP, 10 glucose, 10 HEPES and 0.001 muscimol, 0.001 strychnine pH 7.4. Single-channel events were detected by the half-amplitude threshold criterion at a final bandwith of 1–2 kHz.

Recordings and analysis used pClamp 10.0 (Axon). Liquid junction potentials were not corrected and would introduce maximal shifts of ±2.8 mV.

Eye movement recordings

Vestibulo-ocular reflexes were measured as previously described (Schonewille *et al*, 2010). Mice were head fixed by a surgically preplaced immobilizing construct and positioned in the centre of a turntable, surrounded by a drum with a random dotted pattern (dot size 2°, diameter 63 cm). Mice were subjected to sinusoidal rotation of the drum in light (OKR) or the table in dark (VOR) or light (VVOR) to test performance. On subsequent days, adaptation was induced by mismatching the visual and vestibular stimulation. On training, day 1 both are rotated in phase at the same frequency (0.6 Hz) and amplitude (5°); the next days, the drum amplitude is increased to 7.5° on day 2 to 10° on days 3–5. Mice were kept in the dark overnight in between training sessions. Gain was calculated, after calibrating, averaging and fitting, as the ratio between pupil and stimulus velocity and phase as their timing difference in degrees (Stahl *et al*, 2000; van Alphen *et al*, 2001). Consolidation is the percentage of learned response that is still present the next day. For details, see Supplementary Methods.

Data analysis

Results are presented as means with standard error of mean (s.e.m.), unless stated otherwise. For statistical analyses, repeated measures ANOVA, one-way ANOVA, Student's *t*-test, paired samples Student's *t*-test, and Turkey HSD *post hoc* tests were used as appropriate.

Supplementary data

Supplementary data are available at *The EMBO Journal* Online (http://www.embojournal.org).

Acknowledgements

We thank A von Bock, R Leben, R de Avila Freire, and E Haasdijk for technical assistance; and M Meyer for generously providing L7/Pcp2::Cre mice. Supported by a grant of the Deutsche Forschungsgemeinschaft (DFG) (JE 164/8 and Exc 257 Neuro-Cure) and the Prix Louis-Jeantet de Médecine to TJJ, a stipend from the Alexander von Humboldt Foundation to GS, and a grant of the DFG (HU 800/5-1) to CAH. In addition, we thank the Dutch Organization for Medical Sciences (ZonMw; CIDZ), Life Sciences (ALW; CIDZ, MS), Erasmus University Rotterdam Fellowship (MS), Senter (Neuro-Bsik; CIDZ), Prinses Beatrix Fonds (CIDZ), and the SENSOPAC, CEREBNET and C7 programs of the European Community (CIDZ) for their financial support.

Author contributions: PS and GS performed patch-clamp experiments, PS immunohistochemistry, MS mouse behavioural studies, AB electron microscopy, IK and CAH generated floxed Kcc2 mice, YR generated floxed Kcc3 mice, WW provided Δα6::Cre mice, CAH and TJJ initiated the study, CIDZ and TJJ planned experiments, and GS, PS, MS, TJJ and CIDZ wrote the paper.

Conflict of interest

The authors declare that they have no conflict of interest.

References

Akerman CJ, Cline HT (2006) Depolarizing GABAergic conductances regulate the balance of excitation to inhibition in the developing retinotectal circuit *in vivo*. *J Neurosci* **26:** 5117–5130

Aller MI, Jones A, Merlo D, Paterlini M, Meyer AH, Amtmann U, Brickley S, Jolin HE, McKenzie AN, Monyer H, Farrant M, Wisden W (2003) Cerebellar granule cell Cre recombinase expression. *Genesis* **36:** 97–103

Aller MI, Veale EL, Linden AM, Sandu C, Schwaninger M, Evans LJ, Korpi ER, Mathie A, Wisden W, Brickley SG (2005) Modifying the subunit composition of TASK channels alters the modulation of a leak conductance in cerebellar granule neurons. *J Neurosci* **25:** 11455–11467

Andreescu CE, Milojkovic BA, Haasdijk ED, Kramer P, De Jong FH, Krust A, De Zeeuw CI, De Jeu MT (2007) Estradiol improves cerebellar memory formation by activating estrogen receptor beta. *J Neurosci* **27:** 10832–10839

Andreescu CE, Prestori F, Brandalise F, D'Errico A, De Jeu MT, Rossi P, Botta L, Kohr G, Perin P, D'Angelo E, De Zeeuw CI (2011) NR2A subunit of the N-methyl D-aspartate receptors are required for potentiation at the mossy fiber to granule cell synapse and vestibulo-cerebellar motor learning. *Neuroscience* **176:** 274–283

Armano S, Rossi P, Taglietti V, D'Angelo E (2000) Long-term potentiation of intrinsic excitability at the mossy fiber-granule cell synapse of rat cerebellum. *J Neurosci* **20:** 5208–5216

Barski JJ, Dethleffsen K, Meyer M (2000) Cre recombinase expression in cerebellar Purkinje cells. *Genesis* **28:** 93–98

Ben-Ari Y (2002) Excitatory actions of GABA during development: the nature of the nurture. *Nat Rev Neurosci* **3:** 728–739

Ben-Ari Y, Khazipov R, Leinekugel X, Caillard O, Gaiarsa JL (1997) $GABA_A$, NMDA and AMPA receptors: a developmentally regulated 'ménage à trois'. *Trends Neurosci* **20:** 523–529

Blaesse P, Airaksinen MS, Rivera C, Kaila K (2009) Cation-chloride cotransporters and neuronal function. *Neuron* **61:** 820–838

Boettger T, Rust MB, Maier H, Seidenbecher T, Schweizer M, Keating DJ, Faulhaber J, Ehmke H, Pfeffer C, Scheel O, Lemcke B, Horst J, Leuwer R, Pape HC, Volkl H, Hübner CA, Jentsch TJ (2003) Loss of K-Cl co-transporter KCC3 causes deaf-

ness, neurodegeneration and reduced seizure threshold. *EMBO J* **22:** 5422–5434

Braissant O, Wahli W (1998) Differential expression of peroxisome proliferator-activated receptor-α, -β, and -γ during rat embryonic development. *Endocrinology* **139:** 2748–2754

Brickley SG, Cull-Candy SG, Farrant M (1996) Development of a tonic form of synaptic inhibition in rat cerebellar granule cells resulting from persistent activation of GABAA receptors. *J Physiol* **497:** 753–759

Brickley SG, Revilla V, Cull-Candy SG, Wisden W, Farrant M (2001) Adaptive regulation of neuronal excitability by a voltage-independent potassium conductance. *Nature* **409:** 88–92

Cancedda L, Fiumelli H, Chen K, Poo MM (2007) Excitatory GABA action is essential for morphological maturation of cortical neurons *in vivo*. *J Neurosci* **27:** 5224–5235

Cherubini E, Gaiarsa JL, Ben-Ari Y (1991) GABA: an excitatory transmitter in early postnatal life. *Trends Neurosci* **14:** 515–519

D'Angelo E, Rossi P, Armano S, Taglietti V (1999) Evidence for NMDA and mGlu receptor-dependent long-term potentiation of mossy fiber-granule cell transmission in rat cerebellum. *J Neurophysiol* **81:** 277–287

De Zeeuw CI, Hoebeek FE, Bosman LW, Schonewille M, Witter L, Koekkoek SK (2011) Spatiotemporal firing patterns in the cerebellum. *Nat Rev Neurosci* **12:** 327–344

De Zeeuw CI, Holstege JC, Ruigrok TJ, Voogd J (1989) Ultrastructural study of the GABAergic, cerebellar, and mesodiencephalic innervation of the cat medial accessory olive: anterograde tracing combined with immunocytochemistry. *J Comp Neurol* **284:** 12–35

Duprat F, Lesage F, Fink M, Reyes R, Heurteaux C, Lazdunski M (1997) TASK, a human background K^+ channel to sense external pH variations near physiological pH. *EMBO J* **16:** 5464–5471

Eccles JC, Ito M, Szentagothai J (1967) *The Cerebellum as a Neuronal Machine*. New York: Springer-Verlag

Fricker D, Verheugen JA, Miles R (1999) Cell-attached measurements of the firing threshold of rat hippocampal neurones. *J Physiol* **517:** 791–804

Gabbiani F, Midtgaard J, Knöpfel T (1994) Synaptic integration in a model of cerebellar granule cells. *J Neurophysiol* **72:** 999–1009

Gauvain G, Chamma I, Chevy Q, Cabezas C, Irinopoulou T, Bodrug N, Carnaud M, Levi S, Poncer JC (2011) The neuronal K-Cl cotransporter KCC2 influences postsynaptic AMPA receptor content and lateral diffusion in dendritic spines. *Proc Natl Acad Sci USA* **108:** 15474–15479

Hadley SH, Amin J (2007) Rat α6β2δ $GABA_A$ receptors exhibit two distinct and separable agonist affinities. *J Physiol* **581:** 1001–1018

Hamann M, Rossi DJ, Attwell D (2002) Tonic and spillover inhibition of granule cells control information flow through cerebellar cortex. *Neuron* **33:** 625–633

Hausser M, Clark BA (1997) Tonic synaptic inhibition modulates neuronal output pattern and spatiotemporal synaptic integration. *Neuron* **19:** 665–678

Hoebeek FE, Stahl JS, van Alphen AM, Schonewille M, Luo C, Rutteman M, van den Maagdenberg AM, Molenaar PC, Goossens HH, Frens MA, De Zeeuw CI (2005) Increased noise level of Purkinje cell activities minimizes impact of their modulation during sensorimotor control. *Neuron* **45:** 953–965

Hübner CA, Lorke DE, Hermans-Borgmeyer I (2001a) Expression of the Na-K-2Cl-cotransporter NKCC1 during mouse development. *Mech Dev* **102:** 267–269

Hübner CA, Stein V, Hermans-Borgmeyer I, Meyer T, Ballanyi K, Jentsch TJ (2001b) Disruption of KCC2 reveals an essential role of K-Cl cotransport already in early synaptic inhibition. *Neuron* **30:** 515–524

Jacobs S, Ruusuvuori E, Sipila ST, Haapanen A, Damkier HH, Kurth I, Hentschke M, Schweizer M, Rudhard Y, Laatikainen LM, Tyynelä J, Praetorius J, Voipio J, Hübner CA (2008) Mice with targeted *Slc4a10* gene disruption have small brain ventricles and show reduced neuronal excitability. *Proc Natl Acad Sci USA* **105:** 311–316

Jin X, Huguenard JR, Prince DA (2005) Impaired Cl^- extrusion in layer V pyramidal neurons of chronically injured epileptogenic neocortex. *J Neurophysiol* **93:** 2117–2126

Kaila K, Voipio J (1987) Postsynaptic fall in intracellular pH induced by GABA-activated bicarbonate conductance. *Nature* **330:** 163–165

Kanaka C, Ohno K, Okabe A, Kuriyama K, Itoh T, Fukuda A, Sato K (2001) The differential expression patterns of messenger RNAs encoding K-Cl cotransporters (KCC1,2) and Na-K-2Cl cotransporter (NKCC1) in the rat nervous system. *Neuroscience* **104:** 933–946

Karschin C, Wischmeyer E, Preisig-Müller R, Rajan S, Derst C, Grzeschik KH, Daut J, Karschin A (2001) Expression pattern in brain of TASK-1, TASK-3, and a tandem pore domain K^+ channel subunit, TASK-5, associated with the central auditory nervous system. *Mol Cell Neurosci* **18:** 632–648

Khalilov I, Chazal G, Chudotvorova I, Pellegrino C, Corby S, Ferrand N, Gubkina O, Nardou R, Tyzio R, Yamamoto S, Jentsch TJ, Hübner CA, Gaiarsa J-L, Ben-Ari Y, Medina I (2011) Enhanced synaptic activity and epileptiform events in the embryonic Kcc2 deficient hippocampus. *Front Cell Neurosci* **5:** Article 23

Korpi ER, Kuner T, Seeburg PH, Lüddens H (1995) Selective antagonists for the cerebellar granule cell-specific γ-aminobutyric acid type A receptor. *Mol Pharmacol* **47:** 283–289

Laurie DJ, Seeburg PH, Wisden W (1992) The distribution of 13 $GABA_A$ receptor subunit mRNAs in the rat brain. II. Olfactory bulb and cerebellum. *J Neurosci* **12:** 1063–1076

Lee S, Yoon BE, Berglund K, Oh SJ, Park H, Shin HS, Augustine GJ, Lee CJ (2010) Channel-mediated GABA release from glia. *Science* **330:** 790–796

Li H, Khirug S, Cai C, Ludwig A, Blaesse P, Kolikova J, Afzalov R, Coleman SK, Lauri S, Airaksinen MS, Keinanen K, Khiroug L, Saarma M, Kaila K, Rivera C (2007) KCC2 interacts with the dendritic cytoskeleton to promote spine development. *Neuron* **56:** 1019–1033

Ludwig A, Uvarov P, Soni S, Thomas-Crusells J, Airaksinen MS, Rivera C (2011) Early growth response 4 mediates BDNF induction of potassium chloride cotransporter 2 transcription. *J Neurosci* **31:** 644–649

Mikawa S, Wang C, Shu F, Wang T, Fukuda A, Sato K (2002) Developmental changes in KCC1, KCC2 and NKCC1 mRNAs in the rat cerebellum. *Brain Res* **136:** 93–100

Mittmann W, Hausser M (2007) Linking synaptic plasticity and spike output at excitatory and inhibitory synapses onto cerebellar Purkinje cells. *J Neurosci* **27:** 5559–5570

Pearson MM, Lu J, Mount DB, Delpire E (2001) Localization of the K^+-Cl^- cotransporter, KCC3, in the central and peripheral nervous systems: expression in the choroid plexus, large neurons and white matter tracts. *Neuroscience* **103:** 481–491

Pfeffer CK, Stein V, Keating DJ, Maier H, Rinke I, Rudhard Y, Hentschke M, Rune GM, Jentsch TJ, Hübner CA (2009) NKCC1-dependent GABAergic excitation drives synaptic network maturation during early hippocampal development. *J Neurosci* **29:** 3419–3430

Pugh JR, Jahr CE (2011) Axonal $GABA_A$ receptors increase cerebellar granule cell excitability and synaptic activity. *J Neurosci* **31:** 565–574

Rinehart J, Maksimova YD, Tanis JE, Stone KL, Hodson CA, Zhang J, Risinger M, Pan W, Wu D, Colangelo CM, Forbush B, Joiner CH, Gulcicek EE, Gallagher PG, Lifton RP (2009) Sites of regulated phosphorylation that control K-Cl cotransporter activity. *Cell* **138:** 525–536

Rivera C, Voipio J, Payne JA, Ruusuvuori E, Lahtinen H, Lamsa K, Pirvola U, Saarma M, Kaila K (1999) The K^+/Cl^- co-transporter KCC2 renders GABA hyperpolarizing during neuronal maturation. *Nature* **397:** 251–255

Rossi DJ, Hamann M, Attwell D (2003) Multiple modes of GABAergic inhibition of rat cerebellar granule cells. *J Physiol* **548:** 97–110

Rust MB, Faulhaber J, Budack MK, Pfeffer C, Maritzen T, Didie M, Beck FX, Boettger T, Schubert R, Ehmke H, Jentsch TJ, Hübner CA (2006) Neurogenic mechanisms contribute to hypertension in mice with disruption of the K-Cl cotransporter KCC3. *Circ Res* **98:** 549–556

Santamaria F, Tripp PG, Bower JM (2007) Feedforward inhibition controls the spread of granule cell-induced Purkinje cell activity in the cerebellar cortex. *J Neurophysiol* **97:** 248–263

Saxena NC, Macdonald RL (1996) Properties of putative cerebellar gamma-aminobutyric acid A receptor isoforms. *Mol Pharmacol* **49:** 567–579

Schonewille M, Belmeguenai A, Koekkeok SK, Houtman SH, Boele HJ, van Beugen BJ, Gao Z, Badura A, Ohtsuki G, Amerika WE, Hosy E, Hoebeek FE, Elgersma Y, Hansel C, De Zeeuw CI (2010) Purkinje cell-specific knockout of the protein

phosphatase PP2B impairs potentiation and cerebellar motor learning. *Neuron* **67:** 618–628

Stahl JS, James RA, Oommen BS, Hoebeek FE, De Zeeuw CI (2006) Eye movements of the murine P/Q calcium channel mutant tottering, and the impact of aging. *J Neurophysiol* **95:** 1588–1607

Stahl JS, van Alphen AM, De Zeeuw CI (2000) A comparison of video and magnetic search coil recordings of mouse eye movements. *J Neurosci Methods* **99:** 101–110

Stein V, Hermans-Borgmeyer I, Jentsch TJ, Hübner CA (2004) Expression of the KCl cotransporter KCC2 parallels neuronal maturation and the emergence of low intracellular chloride. *J Comp Neurol* **468:** 57–64

Takayama C, Inoue Y (2006) Developmental localization of potassium chloride co-transporter 2 in granule cells of the early postnatal mouse cerebellum with special reference to the synapse formation. *Neuroscience* **143:** 757–767

Tyzio R, Cossart R, Khalilov I, Minlebaev M, Hubner CA, Represa A, Ben-Ari Y, Khazipov R (2006) Maternal oxytocin triggers a transient inhibitory switch in GABA signaling in the fetal brain during delivery. *Science* **314:** 1788–1792

van Alphen AM, Stahl JS, De Zeeuw CI (2001) The dynamic characteristics of the mouse horizontal vestibulo-ocular and optokinetic response. *Brain Res* **890:** 296–305

Wang C, Shimizu-Okabe C, Watanabe K, Okabe A, Matsuzaki H, Ogawa T, Mori N, Fukuda A, Sato K (2002) Developmental changes in KCC1, KCC2, and NKCC1 mRNA expressions in the rat brain. *Brain Res* **139:** 59–66

Watanabe D, Inokawa H, Hashimoto K, Suzuki N, Kano M, Shigemoto R, Hirano T, Toyama K, Kaneko S, Yokoi M, Moriyoshi K, Suzuki M, Kobayashi K, Nagatsu T, Kreitman RJ, Pastan I, Nakanishi S (1998) Ablation of cerebellar Golgi cells disrupts synaptic integration involving GABA inhibition and NMDA receptor activation in motor coordination. *Cell* **95:** 17–27

Williams JR, Sharp JW, Kumari VG, Wilson M, Payne JA (1999) The neuron-specific K-Cl cotransporter, KCC2. Antibody development and initial characterization of the protein. *J Biol Chem* **274:** 12656–12664

Wulff P, Schonewille M, Renzi M, Viltono L, Sassoe-Pognetto M, Badura A, Gao Z, Hoebeek FE, van Dorp S, Wisden W, Farrant M, De Zeeuw CI (2009) Synaptic inhibition of Purkinje cells mediates consolidation of vestibulo-cerebellar motor learning. *Nat Neurosci* **12:** 1042–1049

Zhu L, Lovinger D, Delpire E (2005) Cortical neurons lacking KCC2 expression show impaired regulation of intracellular chloride. *J Neurophysiol* **93:** 1557–1568

